







Projection Mapping for In-Situ Surgery Planning by the Example of DIEP Flap Breast Reconstruction

J. Martschinke¹ , V. Klein¹ , P. Kurth¹, K. Engel², I. Ludolph³ , T. Hauck³ , R.E. Horch³  and M. Stamminger¹ 

¹Visual Computing, University of Erlangen-Nuremberg (FAU), Germany

²Siemens Healthineers Erlangen, Germany

³Department of Plastic and Hand Surgery and Laboratory for Tissue Engineering and Regenerative Medicine, University Hospital of Erlangen, Germany

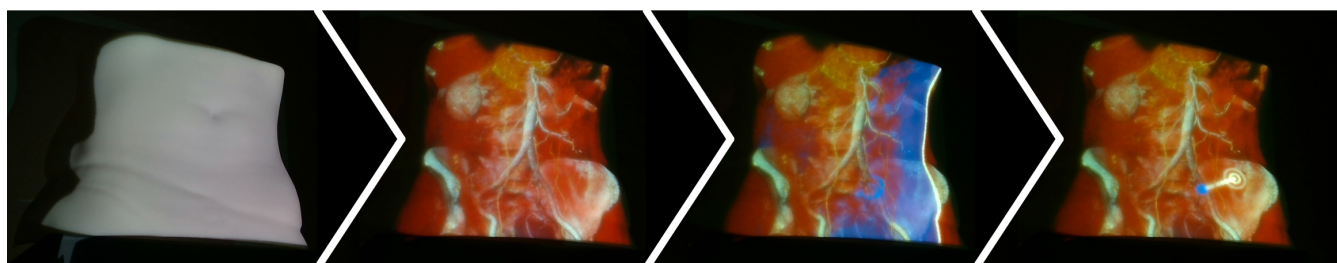


Figure 1: Results of our interactive volumetric visualization pipeline for surgery planning. From left to right: 3D-printed model of the abdomen, volumetric visualization through projection directly onto the skin, plane and cursor for interactive selection of a 3D point in the volume, resulting internal point (blue ball) and corresponding skin point (white concentric circles).

Abstract

Nowadays, many surgical procedures require preoperative planning, mostly relying on data from 3D imaging techniques like computed tomography or magnetic resonance imaging. However, preoperative assessment of this data is carried out on the PC (using classical CT/MR viewing software) and not on the patient's body itself. Therefore, surgeons need to transfer both their overall understanding of the patient's individual anatomy and also specific markers and labels for important points from the PC to the patient only with the help of imaginative power or approximative measurement. In order to close the gap between preoperative planning on the PC and surgery on the patient, we propose a system to directly project preoperative knowledge to the body surface by projection mapping. As a result, we are able to display both assigned labels and a volumetric and view-dependent view of the 3D data in-situ. Furthermore, we offer a method to interactively navigate through the data and add 3D markers directly in the projected volumetric view. We demonstrate the benefits of our approach using DIEP flap breast reconstruction as an example. By means of a small pilot study, we show that our method outperforms standard surgical planning in accuracy and can easily be understood and utilized even by persons without any medical knowledge.

CCS Concepts

• **Applied computing** → Health informatics; • **Computing methodologies** → Ray tracing; **Mixed / augmented reality**;

1. Introduction

In modern plastic and also general surgery, a planning step prior to the actual intervention is crucial for a large amount of operations. Surgery planning typically involves assessment of the three-dimensional data retrieved through imaging techniques like magnetic resonance imaging (MR) and computed tomography (CT), which is by default done by viewing the preoperative data in a standard 2D viewer for volume data. Using sagittal, coronal and axial

views of the data, the surgeon can gain insights on patient-specific conditions and get a feel for the overall spatial relations. For some interventions, surgeons additionally mark points of interest on the patient's skin for later use during the surgery. This transfer step is typically only guided by approximate measurements (e.g. "at about one third of the distance between breast and hip bone", "10 centimetres below the navel") and spatial imagination, and is therefore prone to errors adversely affecting the subsequent operation.

An example for such an operation requiring preoperative planning is an abdominal-based DIEP (deep inferior epigastric perforator) flap breast reconstruction [HSB82, Har88] following cancer-related mastectomy. As the donor vessels supplying the flap with blood are used to reconnect the flap to the patient's circulatory system during the procedure, it is vital for the success of the intervention not to inflict damage upon those vessels. To improve the outcomes of both DIEP flap surgery and also other microvascular reconstructive procedures, in many cases perforator mapping is performed before the intervention. In this preoperative step, the surgeon maps the course of the perforator vessels including special landmarks onto the patient's abdominal skin and marks the according points for later use. Landmarks of interest include entry, exit and branching points of the vessels, and – most importantly – the points where the supplying vessels perforate (i.e. cross) the abdominal muscles and fascia. At the interface of subcutaneous fat and muscle/fascia, the meticulous preparation of the perforator vessels starts and needs to be continued through the muscle with utmost care not to damage them, as this could lead to flap failure. As the individual topography of the perforator vessels differs drastically between patients [VVF02], preoperative perforator mapping is known to reduce complications in DIEP flap breast reconstruction [FORC*16]. There are a number of available modalities to perform perforator mapping, for example ultrasound, computed tomography angiography (CTA) or magnetic resonance angiography (MRA) [PRC*12], with CTA being the gold standard for preoperative imaging in this field [MKC*10, TGB*07]. However, both the localization of the points of interest in the CTA slice stack and the transfer of the 3D information found in the scan to the localization on the patient's skin are not trivial and introduce errors.

In order to solve both problems and to improve on accuracy of surgery planning in general and of perforator mapping in DIEP flap breast reconstruction in particular, we propose a novel method for preoperative data assessment, using projection to alleviate the transfer from the 3D information found in a preoperative CTA view to the patient's body. To this end, we introduce a system to correctly project information onto the body surface using a standard projector. This system is used to project markers corresponding to the internal points selected earlier (using standard software) directly onto the skin. Moreover, we extend the system by viewer tracking and project a ray-traced visualization of the whole volumetric data set onto the skin, creating the illusion of a "look inside" the body at the operation site and making it easier to gain an overall understanding of the spatial relationships. Lastly, we add a method to select 3D points of interest directly on the projection using a Vive controller, rendering marker transfer from a viewing software on the PC to the patient completely obsolete by creating an in-situ planning tool. Our contribution therefore is threefold. We provide

- a system to correctly project markers on a non-planar body (see Section 3),
- an additional volumetric view of the preoperative data visualized on the patient's skin (see Section 4),
- and a method to interactively choose points of interest directly in the volumetric visualization (see Section 5).

By means of a pilot user study with laypersons, we furthermore show that the proposed system greatly improves the accuracy of marker positioning on the skin (see Section 6).

2. Previous Work

Augmented Reality by HMDs for Surgery Planning. In general surgery planning and assistance, augmented reality (AR) is mostly realized through head-mounted displays (HMDs). There is a large body of research on the usage of HMDs [RWQ*20, EVF19, VTZ*20], both see-through like Google Glass and Microsoft HoloLens and non-see-through like HTC Vive, reaching from applications which merely provide information which would normally be presented to the surgeon on a screen [AJAP*20] to applications which create overlays over the patient and thus enrich the surgeon's understanding of the patient's body [GGs*18, PIL*18]. However, HMD-bound methods are often found cumbersome or distracting, and moreover mutually exclusive in microsurgery, where the surgeon needs to view the operation field through a microscope [VRZ*17]. The field of AR for the preparation of DIEP flap breast reconstruction surgery in particular is only just emerging: Bosc et al. [BFP*17] and Wesselius et al. [WML*21] propose methods to visualize the perforators as a hologram overlaid to the patient using a 2D HMD and a HoloLens, respectively. In their approaches, additional markers have to be glued to the skin in order to register the overlay view to the patient.

Augmented Reality by Projection for Surgery Planning. Projection as an alternative to using head-mounted displays for bringing augmented reality to surgical procedures offers the major advantage that there is no need for surgeons to wear a headset. For general preoperative and intra-operative surgery enhancement, the applications of projection range from rather simple approaches merely using the patient as a canvas to prevent focus change between a display and the surgery site [TRM03] to more advanced approaches using coded light [HDR*01, HBD*01] or optical marker tracking systems [GZXZ21] to ensure registration between the patient and the augmenting content. However, to the best of our knowledge none of these approaches includes depth tracking for marker-less object tracking, offers viewer-dependent volumetric visualization or even interactive in-situ placement of labels. For the special case of DIEP flap breast reconstruction, Hummelink et al. [HHH*15, HVM*17, HHSKU19] developed a projection-based method for preoperative perforator mapping. However, they employ a small hand-held projector, offer pure markers instead of a volumetric visualization, and only register the projection to the patient by hand, moving and rotating the projector and checking the resulting projection using a standard ruler [HHH*15]. Chae et al. [CGHSR18] and Sotsuka et al. [SMF*14] propose similar methods, also relying on manual registration using natural features like the navel or additional markers attached to the skin and also not providing interaction with a full volumetric rendering, but only 2D projections overlaid over the patient's skin.

3. System for Marker Projection

Our first contribution is a setup to robustly and accurately project markers found by standard surgery planning at the PC (and subsequently also a full volumetric rendering and additional information, see Sections 4 and 5) onto a patient's skin. The basic setup (see Figure 2) consists of a standard projector, an RGB-D camera and the target object to illuminate.



Figure 2: Setup for our projection system: standard projector (1), 3D print of abdominal skin (2), and RGB-D camera for object tracking and camera-to-projector calibration (3). The Vive tracker (4) and controller (5) will only be used for the extensions depicted in Sections 4 and 5, respectively. The camera position shown here is used for capturing most images of projection results throughout this paper.

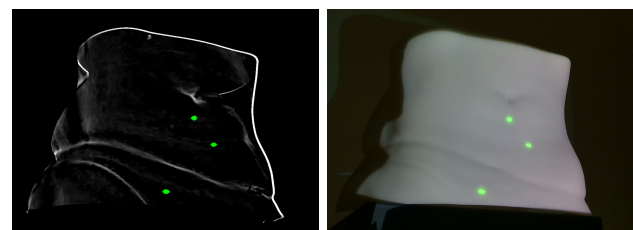
The target object in the DIEP flap breast reconstruction case is the abdominal skin of a patient. During both implementation and evaluation of our method, we used a 3D-printed model of an abdomen as a replacement for a real patient. The 3D print was created using a CTA data set of a real patient and extracting the surface of this volume by applying the Marching Cubes algorithm [LC87].

As a basis for our system, we use a combination of robust multi-projector mapping including depth tracking [SCT*15, LSC*17] with automatic camera-to-projector calibration [KLS*18]. For the sake of simplicity, we only employ a single projector in our setup, but the system can readily be extended by a second projector to facilitate projecting onto differently oriented surface parts.

Using the aforementioned calibration and tracking routines, we position the projector, the target object and the virtual instance, i.e. mesh, of the target object in a common coordinate system attached to the RGB-D camera and ensure accurate registration of the target object and the mesh. As both the calibration routine [KLS*18] and depth tracking [SCT*15] rely on features found in the target object, the abdominal skin (in contrast to feature-rich body regions like head, hands or feet) constitutes a challenging task for our system. We therefore verify correct registration of mesh and object by projecting surface normals to the 3D print and checking proper alignment of the normal visualization to the few discernible surface features, first and foremost the navel, which can also be identified in the depth image. Using this registration routine, we reach striking accuracy in projecting onto the 3D print of the abdomen, as can be seen in Figure 3. In a future setting with permanently mounted

components, the calibration between RGB-D camera and projector will only have to be done once and stay fixed afterwards.

In order to label a point of interest on the patient’s skin, the surgeon selects a 3D point in the CTA data set in a first step, using a standard visualization tool (for example ITK-SNAP [YPCH*06]). The markers set by the surgeon are exported as a label mask registered with the volume data set. In the basic version of our system, we only visualize the surface points corresponding to these internal markers. We first determine the corresponding skin points by computing the projection of the points to the skin along the sagittal axis. These surface points are then visualized on the surface as small green dots (see Figure 3) using our setup. To preserve them for later use during the intervention, the only thing the surgeon now needs to do is mark the points indicated by the green dots using a skin pen. Alternative models for the correspondence between inner point and surface point – other than mere sagittal projection – could easily be integrated.



(a) rendered from the camera’s view (b) projected and captured

Figure 3: Marker projection result of our basic system. The image of the 3D-printed abdominal model including projected green markers captured by the RGB-D camera (b) closely matches the image resulting from rendering the model mesh and markers from the point of view of the camera (a).

4. Extension to Volumetric View

Being able to project markers onto the skin surely is a helpful option to reduce inaccuracy during the transfer of preoperative planning from the PC to the patient, but it neither provides information about the depth of the internal markers nor does it help the surgeon in gaining an overall spatial intuition about the data set. Therefore, we extend our system by the capability to display not only plain marker points, but also a volumetric rendering of the whole data set. Using a volumetric representation rather than a collection of surface meshes extracted from the CTA data set comes with the advantage of being able to interactively adapt the transfer function, which helps in finding certain structures such as crossing points between different types of tissue.

For rendering the internal structures in a volumetric way, we employ direct volume rendering, using a transfer function and illumination model suited for medical imaging [CEGM16, GES*18], but refrain from utilizing a complete Monte-Carlo path-tracing approach and rather opt for a simpler ray casting scheme in order to maintain interactive frame rates. Using a transfer function specially designed for the visualization of the abdominal region, we

obtain good quality without taking global effects into account. Using this trade-off between quality and performance, we reach about 20 frames per second for a projector with a resolution of 1920x1080 pixels on an NVIDIA GeForce RTX 2060, which would not be enough for the use in an HMD, but allows for a smooth user experience in the projected image (see accompanying video for reference).

To achieve the illusion of showing objects *inside* the body, we have to adapt the volumetric rendering to the observer's position. To this end, we extend the basic setup from Section 3 by a Vive tracker, tracked by HTC's Lighthouse system. The tracker is attached to the viewer's forehead by a strap and its position is used to set up the rays for ray casting. The calibration between the basic setup from Section 3 and the Vive tracker is done manually by positioning the tracker in an eye-to-forehead distance to the camera and storing its position and orientation with respect to the camera on a button press.

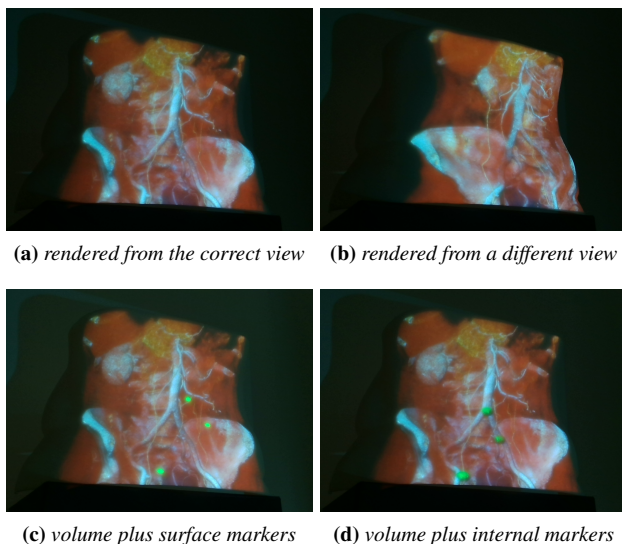


Figure 4: Volumetric projection results. First row: The projection only produces the illusion of looking at the interior of an transparent object when rendered and observed from the same point of view (a), otherwise, distortions impede immersion (b). Second row: With the volumetric extension, it is not only possible to verify the surface markers in a shared volume/marker view (c), but also to visualize the internal markers as volumetric balls.

Using viewer-tracked volumetric rendering, the parallax effect is reproduced correctly for the viewer, creating an immersive experience of being able to look through the skin. Furthermore, the volumetric rendering extension does not only provide a powerful way to gain an overall understanding of the spatial relationships, but also enables us to render the markers from the first surgery planning step as balls embedded into the volumetric scene (see Figure 4d) instead of projecting only the corresponding surface points onto the skin (see Figure 4c). As a result, surgeons can walk around the object and choose the point on the surface belonging to the chosen internal point, using metrics different from plain projection along

the sagittal axis. However, due to the viewer tracking requirement, the volumetric extension of our system can only be used by one surgeon at a time in a meaningful way (see Figure 4a), as distortions occur for viewing angles different from the tracked view (see Figure 4b).

5. Interactive Point Selection

The possibility to project markers found and labeled using a standard CT visualization tool to the skin without the need to use imagination or approximate measurement (see Section 3) greatly improves on accuracy of the transfer step, the option to look at the interior of the body using volumetric rendering (see Section 4) offers a better way to explore the data set and gain an overall intuition about the spatial relationships and vessel courses beneath the abdominal skin. With both the object-tracked and calibrated accurate projection from Section 3 and the viewer-tracked volumetric rendering from Section 4 in place, we can go even further and completely omit the preceding labeling step at the PC by providing a method to directly select landmark points in-situ, therefore adding a Vive controller to the setup to enable interaction with the data set.

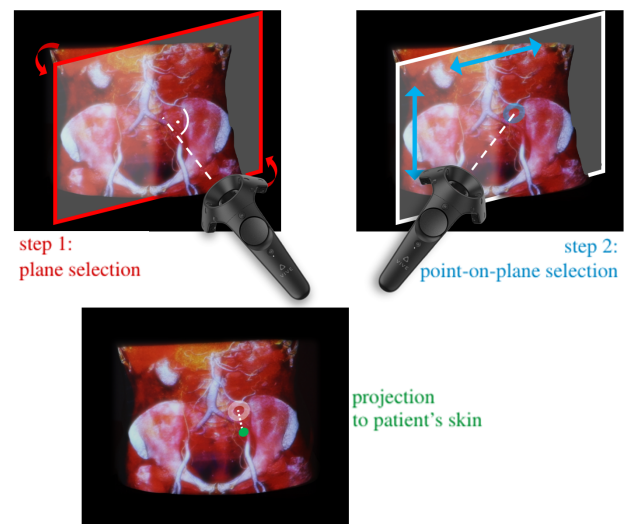


Figure 5: Schematic view of two-step point selection routine and resulting visualization. Please also see the accompanying video for reference.

Two-Step Point Selection. One can think of a number of different possible options for 3D point selection in a volumetric data set using a controller, with the simplest one being a virtual ball attached to the controller at a certain distance, moving synchronously as the user moves the controller. However, first experiments showed that such an approach suffers from inaccuracy due to both trembling and human inability to control a point in three dimensions at the same time. Therefore, we opted for a two-step approach to increase both convenience of the procedure and accuracy of the results. In a first step, the user selects a plane containing the point in question. The plane is attached to the controller at a distance of one meter and orthogonal to its forward axis, is visualized in one of

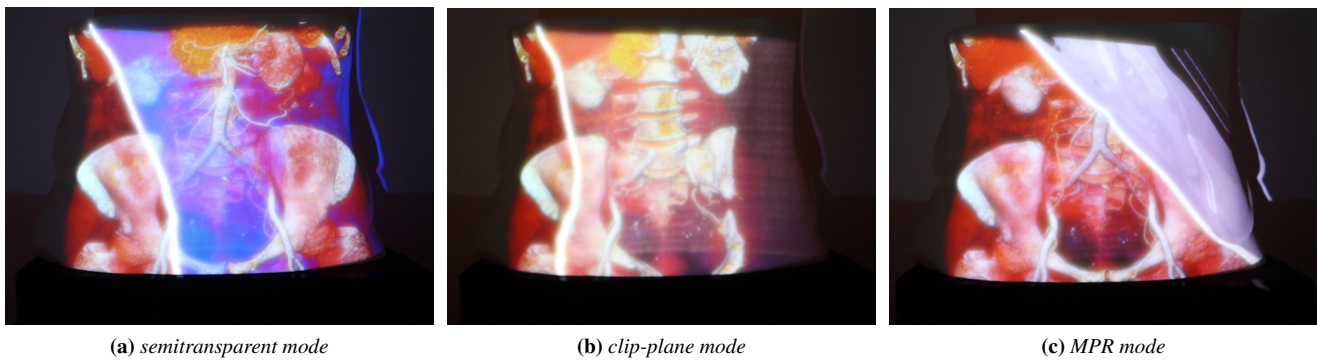


Figure 6: Different plane modes, depicted for different plane orientations: (a) semitransparent mode, (b) clip-plane mode, (c) MPR mode. The plane modes can be toggled using the controller both during plane selection and during point selection, when the position of the plane is already fixed.

three ways (see next paragraph) and can be fixated using a button on the controller. As this plane is not bound to the sagittal, coronal or axial direction, but can move freely in space, it is of superior value for the selection of points (especially on vessels, which naturally follow curved paths not oriented along coordinate axes) than the plane views shown in standard programs. In a second step, the intersection point between the forward axis of the controller and the fixed plane is visualized, which enables the user to select a point on the plane in a laser-pointer fashion. Once the user has marked this point using a button on the controller, both the thusly chosen internal marker point and the corresponding point on the skin are visualized. Figure 5 shows a schematic overview over the two steps and the resulting visualization. With the controller at hand, we furthermore provide a simple way to alter the transfer function in order to assess the different types of tissue in context to each other: By swiping left and right on the trackpad of the controller, the user can change the window leveling and therefore mask out certain tissue types while enhancing others. The full setup and pipeline for in-situ point selection can best be seen in the accompanying video.

Plane Modes. We offer three plane modes with different advantages which can be toggled using the controller. In *semitransparent mode* (see Fig. 6a), the plane is visualized in semitransparent blue. In this mode, the volumetric CTA data can be viewed as a whole without clipping away parts of the volume. When *clip-plane mode* (see Fig. 6b) is selected, the part of the volume in front of the plane is clipped and the plane itself is not shaded at all, giving the user better view on the structures lying exactly on the plane. Lastly, *MPR mode* (see Fig. 6c) shows the multiplanar reconstruction of the CTA data on the current plane in greyscale, also clipping the half-space in front of the plane. This mode introduces occlusion, but in return links the new visualization to the CTA view surgeons might be more familiar with. In all modes, the outline of the volume cross-section is highlighted in white color to provide guidance on the orientation of the plane in space. The user can switch between modes and alter the transfer function at any time during plane selection. For example, one can use the semitransparent mode first to gain an overall understanding of the vessels' paths and find the approximate target region, then switch to clip-plane mode to find the exact location, and lastly verify its correctness using MPR mode.

6. Results

The problem arising during standard perforator mapping and thus the benefit of our method is twofold:

- It is difficult to *select* exact points of interest along vessels (crossing points with muscle layers, branching points etc.) using standard CT viewing software. Our method, however, facilitates the location of such points by providing a volumetric view and the possibility to select planes which are not axis-aligned.
- It is difficult to *transfer* and map a found 3D point to the corresponding point on the patient's abdominal skin for later use during flap extraction. Our method, however, facilitates this transfer by providing a possibility to select a point in-situ and project it directly onto the surface.

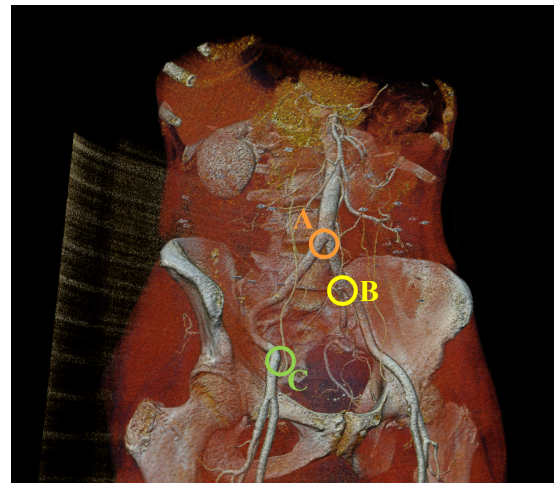


Figure 7: Landmarks to be found and marked by the participants in the three pilot study experiments: branching of aorta in left and right arteria iliaca communis (A), branching of left arteria iliaca communis in arteria iliaca interna and externa (B) and exit point of arteria femoralis from arteria iliaca externa (C). These landmark points are also used for the visualizations found in Figures 3 and 4.

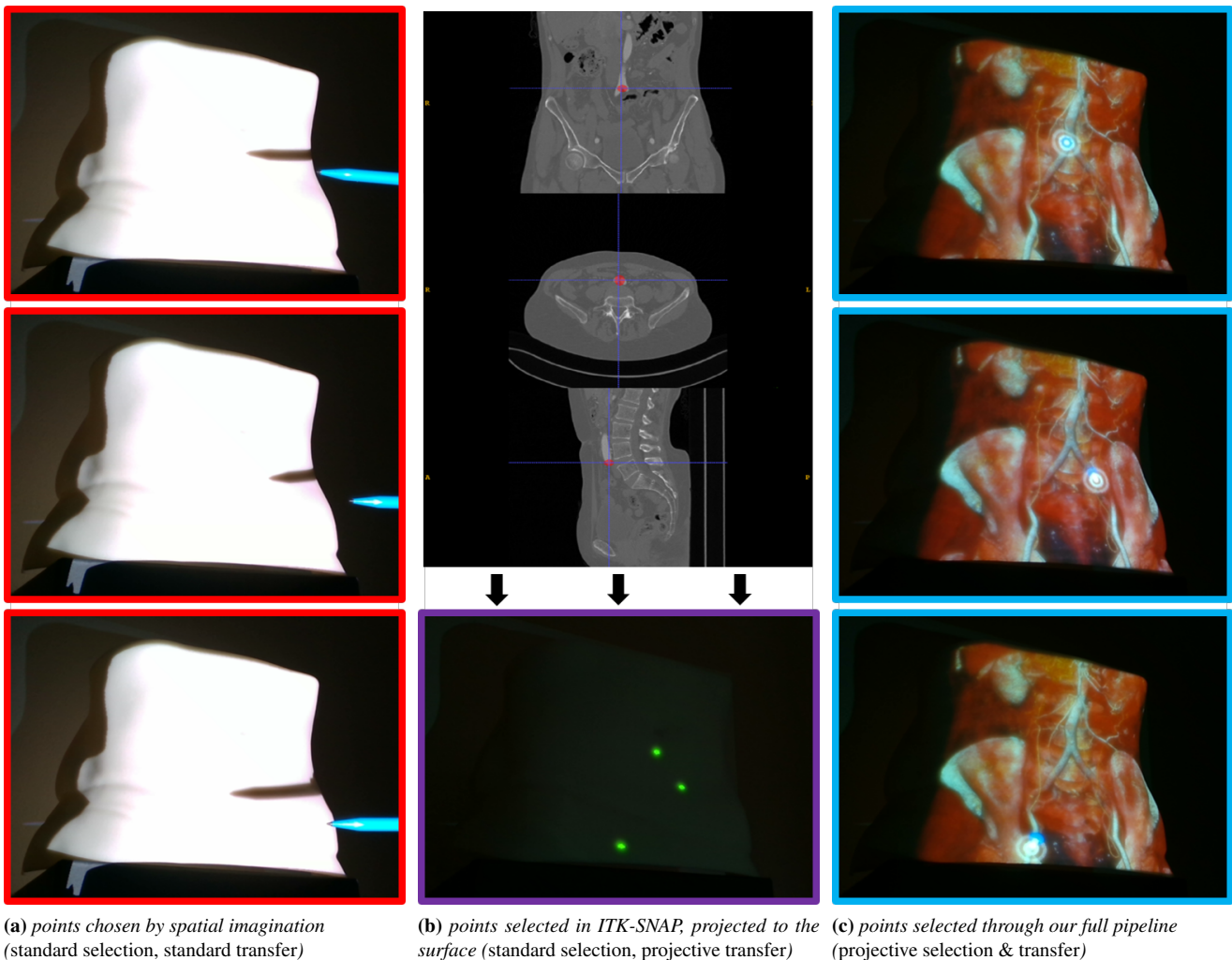


Figure 8: Per-participant results of the pilot user study. For each participant, we store three images of the estimated surface points transferred to the skin in the second task by using only spatial imagination (a), the labeling results from ITK-SNAP and an image showing the markers transferred onto the skin using our projection system (b), and three images captured during the third task showing the surface points selected with our full interactive pipeline (c).

In order to compare the standard routine for perforator mapping to different extents of assistance through our projective system and therefore show its benefit with respect to the two aspects of selection and transfer, we evaluate three variants:

- *standard selection, standard transfer*: Both the selection of the internal point in a standard program and the transfer of this internal marker to the skin surface using only spatial imagination are conducted mimicking the standard perforator mapping routine in the clinical workflow.
- *standard selection, projective transfer*: Selection of the internal points is still done in a standard program, but instead of relying on visual judgment, the transfer step is performed by projecting the markers to the skin using our basic setup (see Section 3).
- *projective selection & transfer*: The internal marker points are selected in-situ using our full projective setup. There is no need

for an extra transfer step as the selection step does not take place in a standard program, but directly on the patient's skin.

To this end, we performed a small pilot user study involving 10 participants (aged 24 to 65; 5 female and 5 male). The participants – all without any medical knowledge – were shown a volumetric rendering of the abdomen (see Figure 7) with three vessel landmarks labeled as points A, B and C. The participants' first task then was to find the respective internal points in a CT stack viewed in a standard program, the second task to find the corresponding points on the patient's skin by means of spatial imagination, like it is done in standard surgery planning routine. In a third task, they were asked to find the same three surface points using our two-step point selection method. Although crossing landmarks (where the according vessels perforate the abdominal muscles) are the most important points for DIEP flap surgery planning, we opted for the

three branching landmarks depicted in Figure 7 to be used in the study instead, as they are easier to identify for medically unexperienced users.

For the first task, we used ITK-SNAP [YPCH*06] as an easy-to-use reference tool for 2D investigation of the CTA volume. Before they were asked to select the landmark points, the participants were shown how to scroll through the volume along the axial, sagittal and coronal axis using the mouse wheel, use the linked cursor to navigate through the views in a connected manner, and mark a point using the labeling tool. Once the participants finished labeling the three points using ITK-SNAP, they were asked to show the corresponding surface points on the abdominal model only using spatial imagination in the second task. For guiding the surface point selection process, the participants were allowed to scroll through the three planar views in ITK-SNAP extensively to assess the spatial relationship between the skin and the markers set by themselves in the previous step, and also look at the original rendering with the landmarks labeled as circles. The per-participant results of these first two tasks were stored as three images taken from the camera's point of view showing the estimated skin points (see Figure 8a, shadow of the pen tip) and, additionally, a label mask exported from ITK-SNAP containing the 3D points selected by the participant. The label mask was fed into our program later on and the participant-set markers were visualized using the simple marker pipeline from Section 3 to differentiate between the errors introduced in the internal marker setting step and in the transfer step of the second task (see Figure 8b).

For the third task, the participants were first given a short introduction into our method, containing the two-step point selection routine and the possibility to switch between the three plane modes. Afterwards, they were asked to select the same three landmarks like in the first two tasks of the experiment. Hereby, they were free to redo the selection steps until they were satisfied with the outcome. The results of this second task were stored as three images taken from the RGB-D camera's point of view showing the results of our method for all three landmarks (see Figure 8c). Due to a technical problem in the recording process, we obtained only 9 images for landmark C.

Figure 8 shows an overview over the intermediate results in the form of seven images per participant. From each of these images, we extract the pixel coordinates of the selected surface points and compare them to the coordinates of the ground truth points obtained by marking the correct point in the standard CTA viewer ITK-SNAP and rendering them from the camera's point of view (see Figure 3a).

Figure 9 depicts the error (i.e. distance to the ground truth surface points) in pixels of the three variants for all participants and landmarks as box plots for a quick overview. Figure 10 offers more precise spatial information by showing the single estimated surface points resulting from the three variants per participant as circles and the ground truth positions as stars.

The results shown in Figures 9 and 10 can be interpreted as follows: As can easily be seen from the left plot in Figure 9, the first variant (*standard selection, standard transfer*) produces by far the largest errors, with an average error of 97 pixels and errors ranging up to 226 pixels. The highest error occurs for landmark C as it is

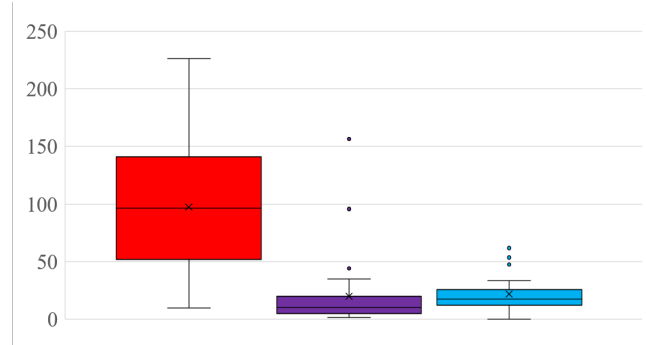


Figure 9: Error computed as Euclidean distance in pixels to the ground truth for the three variants, gathered over all participants and the three landmarks A, B and C. From left to right: standard selection, standard transfer (red); standard selection, projective transfer (purple); projective selection & transfer (blue). The colors of the box plots match the ones used in Figure 8 to illustrate the origin of the measured error values.

farthest away from the navel and other easy-to-incorporate points of reference. The lion's share of this error stems from the transfer step only relying on spatial notion, as is proven by the second plot (*standard selection, projective transfer*) with an average error of only 20 pixels. The third variant (*projective selection & transfer*) shows slightly higher error values in general (average: 23 pixels), but does not exhibit outliers with drastically higher error values like found in the second variant. As shown in Figure 10b, these outliers occur when participants set the internal marker points to a completely wrong location as they cannot recognize the correct landmark points in the standard program, which only offers sagittal, coronal and axial views. Our interactive pipeline, however, visualized the data in a 'natural' way, making it easy for all participants to correctly identify the sought-for internal point. The slightly higher error found in the third variant mostly stems from controller inaccuracy induced by the Vive tracking system. With the arrival of even better tracking hardware in the future, we expect our full method (third variant) to further improve.

Surgeons would likely perform better in the first and second variant, as they are more used to both assessing spatial relationships using only sagittal, coronal and axial view and transferring an internal point to the skin only using their imagination. Using our projection system with direct navigation on the patient, however, even laypersons and less experienced surgeons are able to label landmarks correctly and automatically obtain the correct surface point via projection.

7. Limitations

As it is only possible to account for the position of a single tracked viewer at a time, the system is not suited for a multi-viewer setup. However, the fact that the system was not tested on real patients, but only on a 3D-printed model of the abdominal region, poses the most significant limitation to the current realization of our approach. Future work therefore has to focus on application of our method in an authentic medical environment, implying several challenges: First

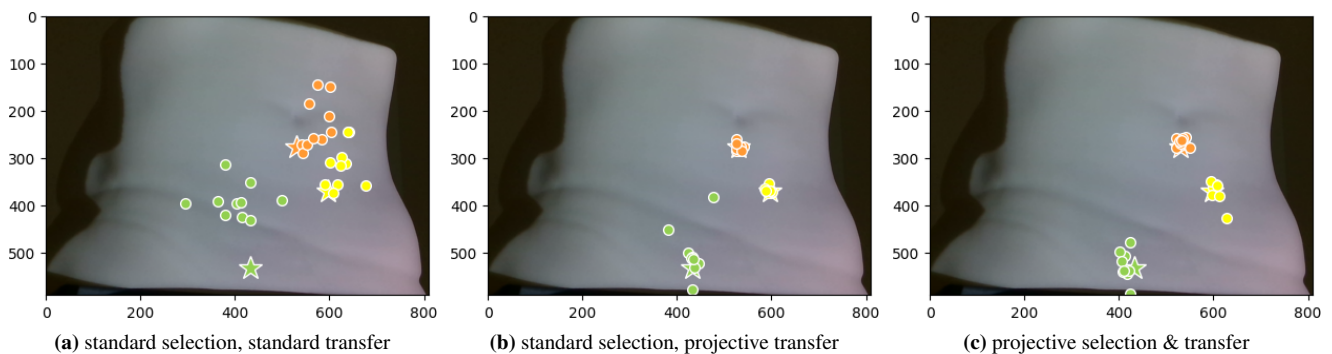


Figure 10: Results for the three target landmarks (visualized as stars) and the three variants from Figure 9. Label colors match the ones used in Figure 7.

of all, real patients, unlike the model used in our experiments, exhibit nonrigid deformation both between recording of the CTA data set and annotation using our system (due to slightly different lying positions) and during the labeling phase (due to breathing and other involuntary movement). Additionally, the current setup needs to be improved to meet the requirements imposed by clinical routine, for example regarding ease of handling and robustness. Further steps towards this goal could be a more convenient realization of viewer tracking and a robust mount for the projector which needs to project vertically upon a lying patient instead of horizontally onto the printed model.

8. Conclusion

In this paper we showed how projection mapping can help with exploring preoperative data and transferring the findings to the real surface in a more intuitive and also more accurate manner. Our system enables even medically inexperienced users to find and mark points of interest in a data set and, more importantly, on the patient's skin, as we could prove in a small pilot study. Thus, we are able to close the gap between standard visualizations for preoperative data and the object to transfer the information to. Once this transfer does not have to be done by the surgeon anymore, we expect more accurate marking on the skin and better surgery results in the long run. Further research can now focus on applying our system to other surgical operations in a variety of intervention fields.

References

- [AJAP*20] AL JANABI H. F., AYDIN A., PALANEER S., MACCHIONE N., AL-JABIR A., KHAN M. S., DASGUPTA P., AHMED K.: Effectiveness of the HoloLens mixed-reality headset in minimally invasive surgery: A simulation-based feasibility study. *Surg Endosc* 34, 3 (2020), 1143–1149. 2
- [BFP*17] BOSCH R., FITOUSSI A., PIGNEUR F., TACHER V., HERSANT B., MENINGAUD J. P.: Identification of perforating vessels by augmented reality: Application for the deep inferior epigastric perforator flap. *Ann Chir Plast Esthet* 62, 4 (2017), 336–339. 2
- [CEGM16] COMANICIU D., ENGEL K., GEORGESCU B., MANSI T.: Shaping the future through innovations: From medical imaging to precision medicine. *Med Image Anal* 33 (2016), 19–26. 3
- [CGHSR18] CHAE M., GANHEWA D., HUNTER-SMITH D., ROZEN W.: Direct Augmented Reality Computed Tomographic Angiography Technique (ARC): An Innovation in Preoperative Imaging. *Eur J Plast Surg* 41 (2018), 415–420. 2
- [EVF19] ECKERT M., VOLMERG J. S., FRIEDRICH C. M.: Augmented reality in medicine: Systematic and bibliographic review. *JMIR Mhealth Uhealth* 7, 4 (2019), e10967. 2
- [FORC*16] FITZGERALD O'CONNOR E., ROZEN W. M., CHOWDHRY M., BAND B., RAMAKRISHNAN V. V., GRIFFITHS M.: Preoperative computed tomography angiography for planning DIEP flap breast reconstruction reduces operative time and overall complications. *Gland Surg* 5, 2 (2016), 93–98. 2
- [GES*18] GLEMSER P. A., ENGEL K., SIMONS D., STEFFENS J., SCHLEMMER H. P., ORAKCIOGLU B.: A New Approach for Photorealistic Visualization of Rendered Computed Tomography Images. *World Neurosurg* 114 (2018), e283–e292. 3
- [GGS*18] GREGORY T. M., GREGORY J., SLEDGE J., ALLARD R., MIR O.: Surgery guided by mixed reality: Presentation of a proof of concept. *Acta Orthop* 89, 5 (2018), 480–483. 2
- [GZXX21] GAO Y., ZHAO Y., XIE L., ZHENG G.: A Projector-Based Augmented Reality Navigation System for Computer-Assisted Surgery. *Sensors (Basel)* 21, 9 (2021), 2931. 2
- [Har88] HARTRAMPF C. R.: The transverse abdominal island flap for breast reconstruction. A 7-year experience. *Clin Plast Surg* 15, 4 (1988), 703–716. 2
- [HBD*01] HOPPE H., BRIEF J., DÄUBER S., RACZKOWSKY J., HAS-SFELD S., WÖRN H.: Projector based intraoperative visualization of surgical planning data. *Computer aided surgery* 6, 4 (2001), 232. 2
- [HDR*01] HOPPE H., DÄUBER S., RACZKOWSKY J., WÖRN H., MOCTEZUMA J. L.: Intraoperative visualization of surgical planning data using video projectors. *Stud Health Technol Inform* 81 (2001), 206–208. 2
- [HHH*15] HUMMELINK S., HAMEETEMAN M., HOOGEVEEN Y., SLUMP C., ULRICH D., SCHULTZE KOOL L.: Preliminary results using a newly developed projection method to visualize vascular anatomy prior to diep flap breast reconstruction. *Journal of Plastic, Reconstructive and Aesthetic Surgery* 68, 3 (2015), 390–394. 2
- [HHSKU19] HUMMELINK S., HOOGEVEEN Y. L., SCHULTZE KOOL L. J., ULRICH D. J. O.: A New and Innovative Method of Preoperatively Planning and Projecting Vascular Anatomy in DIEP Flap Breast Reconstruction: A Randomized Controlled Trial. *Plast Reconstr Surg* 143, 6 (2019), 1151e–1158e. 2
- [HSB82] HARTRAMPF C. R., SCHEFLAN M., BLACK P. W.: Breast reconstruction with a transverse abdominal island flap. *Plast Reconstr Surg* 69, 2 (1982), 216–225. 2

- [HVM*17] HUMMELINK S., VERHULST A. C., MAAL T. J. J., HOOGEVEEN Y. L., SCHULTZE KOOL L. J., ULRICH D. J. O.: An innovative method of planning and displaying flap volume in DIEP flap breast reconstructions. *J Plast Reconstr Aesthet Surg* 70, 7 (2017), 871–875. [2](#)
- [KLS*18] KURTH P., LANGE V., SIEGL C., STAMMINGER M., BAUER F.: Auto-calibration for dynamic multi-projection mapping on arbitrary surfaces. *IEEE Transactions on Visualization and Computer Graphics* 24, 11 (2018), 2886–2894. [3](#)
- [LC87] LORENSEN W. E., CLINE H. E.: Marching cubes: A high resolution 3D surface construction algorithm. In *Proceedings of the 14th Annual Conference on Computer Graphics and Interactive Techniques* (1987), SIGGRAPH '87, Association for Computing Machinery, p. 163–169. [3](#)
- [LSC*17] LANGE V., SIEGL C., COLAIANNI M., STAMMINGER M., BAUER F.: Robust blending and occlusion compensation in dynamic multi-projection mapping. In *Proceedings of the European Association for Computer Graphics: Short Papers* (2017), EG '17, Eurographics Association, p. 1–4. [3](#)
- [MKC*10] MASIA J., KOSUTIC D., CLAVERO J. A., LARRANAGA J., VIVES L., PONS G.: Preoperative computed tomographic angiogram for deep inferior epigastric artery perforator flap breast reconstruction. *J Reconstr Microsurg* 26, 1 (2010), 21–28. [2](#)
- [PIL*18] PRATT P., IVES M., LAWTON G., SIMMONS J., RADEV N., SPYROPOULOU L., AMIRAS D.: Through the HoloLens™ looking glass: Augmented reality for extremity reconstruction surgery using 3D vascular models with perforating vessels. *Eur Radiol Exp*, 1 (2018), 2. [2](#)
- [PRC*12] PRATT G. F., ROZEN W. M., CHUBB D., ASHTON M. W., ALONSO-BURGOS A., WHITAKER I. S.: Preoperative imaging for perforator flaps in reconstructive surgery: A systematic review of the evidence for current techniques. *Ann Plast Surg* 69, 1 (2012), 3–9. [2](#)
- [RWQ*20] RAHMAN R., WOOD M. E., QIAN L., PRICE C. L., JOHNSON A. A., OSGOOD G. M.: Head-Mounted Display Use in Surgery: A Systematic Review. *Surg Innov* 27, 1 (2020), 88–100. [2](#)
- [SCT*15] SIEGL C., COLAIANNI M., THIES L., THIES J., ZOLLHÖFER M., IZADI S., STAMMINGER M., BAUER F.: Real-time pixel luminance optimization for dynamic multi-projection mapping. *ACM Trans. Graph.* 34, 6 (2015), 1–11. [3](#)
- [SMF*14] SOTSUKA Y., MATSUDA K., FUJITA K., FUJIWARA T., KAKIBUCHI M.: Image overlay of deep inferior epigastric artery in breast reconstruction. *Plast Reconstr Surg Glob* 2, 10 (2014), e235. [2](#)
- [TGB*07] TREGASKISS A. P., GOODWIN A. N., BRIGHT L. D., ZIEGLER C. H., ACLAND R. D.: Three-dimensional CT angiography: a new technique for imaging microvascular anatomy. *Clin Anat* 20, 2 (2007), 116–123. [2](#)
- [TRM03] TARDIF J.-P., ROY S., MEUNIER J.: Projector-based augmented reality in surgery without calibration. In *International Conference of the IEEE Engineering in Medicine and Biology Society* (2003), vol. 1, pp. 548–551. [2](#)
- [VRZ*17] VAVRA P., ROMAN J., ZONCA P., IHNAT P., NEMEC M., KUMAR J., HABIB N., EL-GENDI A.: Recent Development of Augmented Reality in Surgery: A Review. *J Healthc Eng* 2017 (2017), 4574172. [2](#)
- [VTZ*20] VLES M. D., TERNG N. C. O., ZIJLSTRA K., MUREAU M. A. M., CORTEN E. M. L.: Virtual and augmented reality for preoperative planning in plastic surgical procedures: A systematic review. *J Plast Reconstr Aesthet Surg* 73, 11 (2020), 1951–1959. [2](#)
- [VVF02] VANDEVOORT M., VRANCKX J. J., FABRE G.: Perforator topography of the deep inferior epigastric perforator flap in 100 cases of breast reconstruction. *Plast Reconstr Surg* 109, 6 (2002), 1912–1918. [2](#)
- [WML*21] WESSELIUS T. S., MEULSTEE J. W., LUIJTEN G., XI T., MAAL T. J. J., ULRICH D. J. O.: Holographic Augmented Reality for DIEP Flap Harvest. *Plast Reconstr Surg* 147, 1 (2021), 25e–29e. [2](#)
- [YPCH*06] YUSHKEVICH P. A., PIVEN J., CODY HAZLETT H., GIMPEL SMITH R., HO S., GEE J. C., GERIG G.: User-guided 3D active contour segmentation of anatomical structures: Significantly improved efficiency and reliability. *Neuroimage* 31, 3 (2006), 1116–1128. [3](#), [7](#)